A Barotropic Model of the Interaction between the Hadley Cell and a Rossby Wave

ISAAC M. HELD AND PETER J. PHILLIPS

Geophysical Fluid Dynamics Laboratory/NOAA, Princeton, New Jersey

(Manuscript received 6 February 1989, in final form 12 October 1989)

ABSTRACT

A barotropic model is described that is designed to study the interaction of the Hadley cell with a Rossby wave forced in midlatitudes by a stationary "topographic" source. The Hadley cell is driven by a mass source/sink that is partly fixed, representing solar heating, and partly dependent on the layer thickness, representing infrared cooling. The response of the mean zonal and meridional winds to infinitesimal wave forcing is analyzed in detail; then the forcing is gradually increased to examine the departures from linearity.

1. Introduction

The subtropical jet is maintained through competition between the acceleration of the westerlies by the poleward flow in the Hadley cell and their deceleration due to the divergence of the eddy momentum flux in low latitudes (e.g., Palmen and Newton 1969, pp. 16–20). The divergence of eddy momentum flux in turn is a direct consequence of mixing of potential vorticity by Rossby waves propagating into the tropics from midlatitudes (e.g., Edmon et al. 1980). If this Rossby wave drag is very small, and if the vertical mixing of momentum is also insignificant, the poleward flow in the Hadley cell will conserve its angular momentum. The angular momentum-conserving flow continues poleward up to a latitude determined by the thermal forcing (Schneider 1977; Held and Hou 1980), resulting in a strong subtropical jet. Significant Rossby wave drag is needed to produce a realistic wind distribution and a realistic momentum budget in the subtropics, in which $fv \approx$ (eddy momentum flux divergence) rather than $(f - \partial u/\partial y)v \approx 0$.

In this study, a simple model of the interaction between the Hadley cell and an incoming Rossby wave is described. The starting point is an idealized shallow-water axisymmetric Hadley cell forced by "solar heating" (a specified mass source) and "infrared cooling" (a mass sink dependent on thickness). A stationary Rossby wave is then forced from midlatitudes. The analysis focuses on the distribution of the vorticity transport and mean flow deceleration caused by the wave, and the effect of this drag on the Hadley cell and the subtropical jet. Only an incoming stationary wave is considered in this study, rather than a stationary wave plus a spectrum of transient waves as seen in the atmosphere, and it should be borne in mind that a broader incoming phase speed spectrum could behave differently. The stationary wave problem is relatively easy to analyze and it is also of interest in its relation to models of the Charney–Devore (1979) type. Calculations with a similar model, but in a different parameter range chosen to examine problems in stratospheric dynamics, have recently been described by Juckes (1989).

Corresponding author address: Dr. Isaac Held, Geophysical Fluid Dynamics Laboratory, Princeton University, P.O. Box 308, Princeton, NJ 08542.

2. The Hadley cell model

Consider the following set of shallow water equations for axisymmetric flow on the sphere:

$$\partial_t U = (f + Z)V - \kappa_M U, \tag{1a}$$

$$\partial_t V = -(f + Z)U - a^{-1}\partial_\theta(\Phi + U^2/2) - \kappa_M V,$$

$$= -fU - a^{-1}U^2 \tan(\theta) - a^{-1}\partial_\theta\Phi - \kappa_M V, \tag{1b}$$

$$\partial_t\Phi = -\Phi_0(a\cos(\theta))^{-1}\partial_\theta(\cos(\theta)V) - \kappa_T(\Phi - \Phi_e(\theta)),$$

$$Z \equiv -(a\cos(\theta))^{-1}\partial_\theta(\cos(\theta)U),$$

$$f \equiv 2\Omega\sin(\theta). \tag{1c}$$

The term $\kappa_T(\Phi - \Phi_e)$ is the mass source/sink, where Φ_e is given the simple form

$$\Phi_e(\theta) = -\frac{2}{3}\Delta_\Phi P_2(\cos(\theta)). \tag{2}$$

Here P_2 the second Legendre polynomial and Δ_Φ the difference in the geopotential from equator to pole in "radiative-convective equilibrium." Rayleigh friction proportional to κ_M, which can be thought of as representing vertical mixing, has been included in the momentum equations. The very small term proportional to $\partial_\theta V^2$ has been omitted in (1b). More importantly,

any momentum source associated with the mass source has been omitted.

There are two distinct ways of motivating the use of such a barotropic model for a study of the Hadley cell and the subtropical jet, neither of which is entirely satisfactory. Consider first an isentropic layer of the atmosphere, with potential temperature Θ_A, depicted in Fig. 1. The flow within the layer is hydrostatic and independent of height. The layer is bounded above by a "rigid" surface whose pressure is a function of latitude $P_T(\theta)$. The fluid underneath this layer has the potential temperature Θ_B. For axisymmetric flow in such a layer, the momentum equations in pressure coordinates are just as in (1), once again ignoring any "vertical" flux of momentum associated with the mass source. Since P_T is assumed to be fixed, conservation of mass results in the following equation for the pressure at the lower boundary P_B:

$$\partial_t P_B = -(a\cos(\theta))^{-1}\partial_\theta(\cos(\theta)(P_B - P_T)V) + (\text{source/sink}). \quad (3)$$

By integrating the hydrostatic equation

$$\partial\Phi/\partial(p/p_*)^\kappa = -c_p\Theta \quad (4)$$

across the lower interface and assuming that the geopotential gradient in the lower layer is negligible, one obtains a relationship between the gradients of P_B, or of $\Pi_B \equiv c_p(P_B/P_*)^\kappa$, and Φ:

$$\nabla\Phi = (\Theta_A - \Theta_B)\nabla\Pi_B. \quad (5)$$

In geostrophic balance, $U = (fa)^{-1}\partial\Phi/\partial\theta$; if this zonal wind field is to approximate the observed winds in the upper troposphere, and if Θ_A and Θ_B are chosen to represent the upper and lower troposphere, then the slope of the lower boundary of the layer will have to approximate the observed mean tropospheric isentropic slope. However, one also wants this layer to represent the outflow from the Hadley cell. Unfortunately, these conditions are mutually exclusive: an isentropic layer that lies between 300 and 100 mb in the tropics, so as to be representative of the Hadley cell outflow, lies above the tropopause in high latitudes, so the slope of its lower boundary will not be representative of the troposphere. A one-layer model of the upper troposphere should be thought of as having heuristic value only; it may miss important dynamics associated with the fact that isentropic surfaces of interest intersect the tropopause.

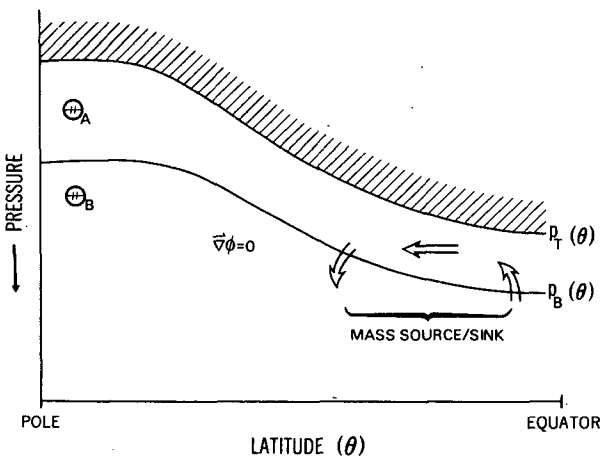

FIG. 1. Schematic of the one-layer model.

To obtain a linear shallow water height equation of the form (1c), one must ignore the nonlinearity that enters through the relation between Π_B and P_B, and one must ignore variations in $P_B - P_T$ in the computation of the mass flux convergence. We can set

$$\frac{\partial\phi}{\partial t} = (\Theta_A - \Theta_B)\frac{\partial\Pi_B}{\partial t} = (\Theta_A - \Theta_B)\frac{\partial\Pi_B}{\partial P_B}\frac{\partial P_B}{\partial t}. \quad (6)$$

The analogue of Φ_0 is then

$$(\Theta_A - \Theta_B)(\partial\Pi/\partial p)_B(P_B - P_T). \quad (7)$$

For a description of a shallow water model in which the nonlinearity associated with the term $\partial\Pi/\partial p$ is retained, see Salby (1989). To justify the neglect of variations in $P_B - P_T$, one can formally consider a layer, as pictured in Fig. 1, in which the slope of the upper boundary approximately matches the slope of the lower boundary needed to produce winds of the appropriate magnitude.

Alternatively, one can take as a starting point a two-level primitive equation model, such as that in Held and Suarez (1978). For steady axisymmetric flow, an equation analogous to (1) can be obtained by assuming that the lower layer zonal wind is negligible compared with that in the upper layer. For finite-differencing as in Held and Suarez, geostropic balance for the upper layer zonal wind can be written

$$fU_1 = (\Pi_2 - \Pi_1)\frac{1}{a}\frac{\partial\bar{\Theta}}{\partial\theta}, \quad (8)$$

if $U_2 \ll U_1$, where the subscripts 1 and 2 refer to the upper and lower layers, and $\bar{\Theta}$ is the mean potential temperature $\frac{1}{2}(\Theta_1 + \Theta_2)$. The equation for $\bar{\Theta}$ takes the form

$$0 = \frac{\partial\bar{\Theta}}{\partial t} = -\frac{1}{a\cos(\theta)}\frac{\partial}{\partial\theta}(\cos(\theta)V\hat{\Theta}) + \text{forcing}, \quad (9)$$

where $\hat{\Theta} = (\Theta_1 - \Theta_2)/2$, so the role of Φ_0 is played by $(\Pi_2 - \Pi_1)\hat{\Theta}$, in close analogy with (7). One must also ignore the vertical advection of momentum to obtain a system analogous to (1). The limitations of this approach to justifying a shallow water model of the upper troposphere result from the familiar limitations of the two-level model.

One cannot expect to generate a realistic Hadley cell without taking the effects of moisture into account. Where there is upper level divergence there must also be upward motion and low-level convergence, and the latent heat release associated with the resulting water vapor convergence must be thought of as a mass source for the "warm," high Θ layer in the upper troposphere.Where there is lower layer divergence, evaporated water vapor is removed that would otherwise have precipitated, providing a cooling, or mass sink for the high Θ layer. Including a mass source proportional to the divergence is equivalent to a reduction in the value of Φ_0, or of the static stability $\hat{\Theta}$ in the context of the two-layer model. See Neelin and Held (1987) for further discussion of this familiar idea in the context of models of the time-mean tropical flow. It would be natural to choose the resulting effective layer thickness Φ_0 to be very small in the tropics but growing to larger values at higher latitudes; however, the choice here is to retain the simplicity of the model (1a–c) with constant Φ_0, selecting a small value meant to be relevant for the low latitudes where attention will be focused.

If one chooses $P_B = 300$ mb, $P_T - P_B = 200$ mb, and $\Theta_A - \Theta_B = 30$ K, as an example, then (7) implies that $\Phi_0 \approx 4 \times 10^3$ m^2 s^{-2}. This value must then be reduced to take the effects of moisture into account. The value $\Phi_0 = 1 \times 10^3$ is chosen in all calculations described below.

One is tempted to use this barotropic model despite its deficiencies because its qualitative behavior is very similar to that of the fully two-dimensional Hadley cell model analyzed by Held and Hou. As $\kappa_M \to 0$, the solution for U approaches a limit that is independent of Φ_0 and κ_T. Equatorward of the latitude θ_H, this limit is the momentum conserving profile $U_M \equiv \Omega a \sin^2(\theta)/\cos(\theta)$, for which $f + Z = 0$; poleward of θ_H, U approaches its radiative equilibrium value $U_e = -f^{-1}\partial_\theta \Phi_e$. The latitude θ_H is determined completely by $\Phi_e(\theta)$, for given Ω and a. The meridional flow V vanishes for $\theta > \theta_H$ as $\kappa_M \to 0$, and approaches a limit proportional to κ_T/Φ_0 for $\theta < \theta_H$. As κ_M increases, Z eventually becomes negligible as compared with f and the problem becomes linear. Essentially identical models are considered by Hou (1984) for the atmosphere of Venus, by Schneider (1983) for Mars, and by Held and Hoskins (1985) for the terrestrial case.

Figure 2 displays the steady solution to (1) with the following parameter settings:

$$\Phi_0 = 10^3 \text{ m}^2 \text{ s}^{-2}, \quad \Delta_\Phi = 2.0 \times 10^4 \text{ m}^2 \text{ s}^{-2},$$

$$\kappa_T^{-1} = 10 \text{ days}, \quad \Omega = 2\pi/\text{day}, \quad a = 6.4 \times 10^6 \text{ m},$$

$$\kappa_M^{-1} = 5, 10, 20 \text{ and } 40 \text{ days}. \qquad (10)$$

If one ignores the very small dissipative term in (1b), it is easily shown that the steady state U depends on Φ_0, κ_T, and κ_M only through the combination $\Phi_0 \kappa_M \kappa_T^{-1}$.

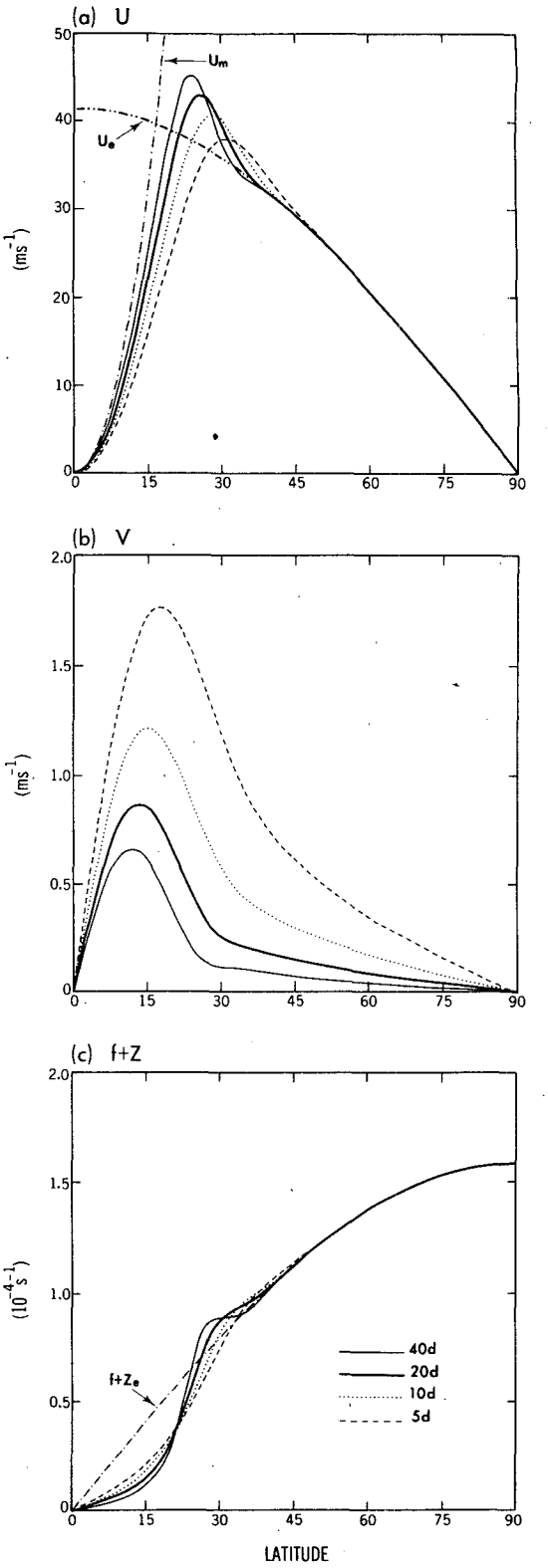

FIG. 2. (a) The zonal wind, (b) meridional wind, and (c) absolute vorticity obtained from the Hadley cell model with $\kappa_M^{-1} = 5$, 10, 20, and 40 days.

The zonal flow for $\Phi_0 = 4 \times 10^3\ m^2\ s^{-2}$ and $\kappa_M^{-1} = 20$ days, for example, is essentially identical to that for $\Phi_0 = 10^3$ and $\kappa_M^{-1} = 5$ (the meridional flow is a factor of 4 smaller).

The form (2) for Φ_e is chosen for simplicity and for consistency with Held and Hou, but it ignores two effects that make the Hadley cell stronger. As Lindzen and Hou (1988) emphasize, the circulation can increase in strength dramatically when a cross-equatorial flow is generated by choosing Φ_e asymmetric about the equator. Equally important, it is not correct to drive the Hadley cell with forcing that varies on such a large latitudinal scale as does the choice (2). The value of Δ_Φ has been chosen to produce winds of roughly the observed magnitude, so in a sense some of the effects of baroclinic eddies have been taken into account in this choice. However, reducing Δ_Φ decreases the strength of the circulation, whereas in reality baroclinic eddies cool the atmosphere strongly in the subtropics, but not in low latitudes, thereby increasing the gradient between the deep tropics and the subtropics that drive the Hadley cell. To help compensate for these omissions, we have chosen a value for the thermal damping, κ_T, that is stronger than can be easily justified for the troposphere; Δ_Φ is also somewhat larger than observed in the upper troposphere.

3. The Rossby wave model

To construct a model of a Rossby wave interacting with this Hadley cell, (1a) is replaced with the nonlinear barotropic vorticity equation

$$\partial_t \zeta = -\nabla \cdot [(f + \zeta + F)\mathbf{v}] - \kappa\zeta - \nu\nabla^4\zeta. \quad (11)$$

The deviations from zonal symmetry are taken to be nondivergent. Thus, the flow v on the RHS of (11) is of the form

$$(u, v) = (-a^{-1}\partial_\theta\psi, (a\cos(\theta))^{-1}\partial_\lambda\psi + V), \quad (12)$$

where $\zeta = \nabla^2\psi$. Scale-selective diffusion has been included in (11) to absorb any enstrophy cascade that occurs. The wave is forced by the steady contribution to the potential vorticity F, which we write as $F = fh'$ where h' can be thought of as the perturbation in the lower boundary divided by the mean layer thickness. (We use fh' rather than $(f + \zeta)h'$ since the forcing is confined to midlatitudes, where $f \gg \zeta$ in any case.) The forcing is given a wavenumber 3 zonal structure and a Gaussian meridional structure:

$$h' = h_0 \exp(-[(\theta - \theta_0)/\Delta_\theta]^2)\cos(\theta)\cos(3\lambda) \quad (13)$$

with $\theta_0 = 45°$N and $\Delta_\theta = 10°$. The $\cos(\theta)$ factor is included to ensure that F is identically zero at the pole.

Equations (1b) and (1c) for V and Φ are unchanged. Since no eddy term has been included in the height equation, V should now be interpreted as the "residual" mean meridional circulation [Andrew and McIntyre (1976); see Andrews (1983) for the isentropic coordinate version]. The model's Eulerian mean meridional circulation can be thought of as equal to $V + \overline{v'h'}$. The Appendix describes the assumptions needed to make this identification precise.

The zonal mean of the vorticity equation now yields

$$\partial_t U = (f + Z)V + \overline{v'q'} - \kappa_M U + (\text{diffusion}), \quad (14)$$

where a prime denotes a deviation from the zonal mean and $q' = \zeta' + fh'$ is the eddy potential vorticity. The effect of the eddies on the zonal mean flow is felt through the momentum flux convergence and the "mountain torque" or "form drag," whose sum is the eddy potential vorticity flux:

$$\overline{v'q'} = \overline{v'\zeta'} + f\overline{v'h'} = -\partial_y(\overline{u'v'}) + f\overline{v'h'}. \quad (15)$$

The choice not to consider the full asymmetric shallow water equations is partly based on the assumption that the divergence in the waves plays a secondary role in the wave breaking and in the resulting mean flow modification. The choice is also influenced by the small value chosen for Φ_0. The special dynamics that can occur in a divergent model when U^2/Φ_0 exceeds unity do not seem germane to the problems being addressed. In addition, the small value of Φ_0 has been justified by arguing that upper level divergence is associated with lower tropospheric convergence and latent heat release. Unlike the divergent axisymmetric Hadley flow, it is not self-evident that divergence accompanying a Rossby wave propagating into low latitudes should be associated with lower tropospheric convergence.

4. The linear Rossby wave limit

Figure 3a shows the stationary wave streamfunction that forms in this system for infinitesimal forcing ($h_0 \to 0$). The parameters are as in (10) with $\kappa_M^{-1} = 20$ days and with the biharmonic diffusion coefficient $\nu = 10^{15}\ m^4\ s^{-1}$. The calculations are performed using a spectral model with R60 truncation.

The solution has a different character north and south of the source. To the north, the solution has very little phase variation with latitude, indicative of a standing wave created by reflection from the wave's polar turning point. To the south, the solution has the phase tilt of a wave propagating equatorwards, indicating that the wave incident on the tropics has been at least partially absorbed. Amplitudes in the Southern Hemisphere are small.

The small wave amplitudes near 30°N are suggestive of partial reflection. A plot of the correlation coefficient between u' and v' can be used to estimate the reflection coefficient. If the solution is approximately of WKB form,

$$\psi \approx \text{Re}\{A[\exp(-iX) + R\exp(iX)]\exp(ikx)\} \quad (16)$$

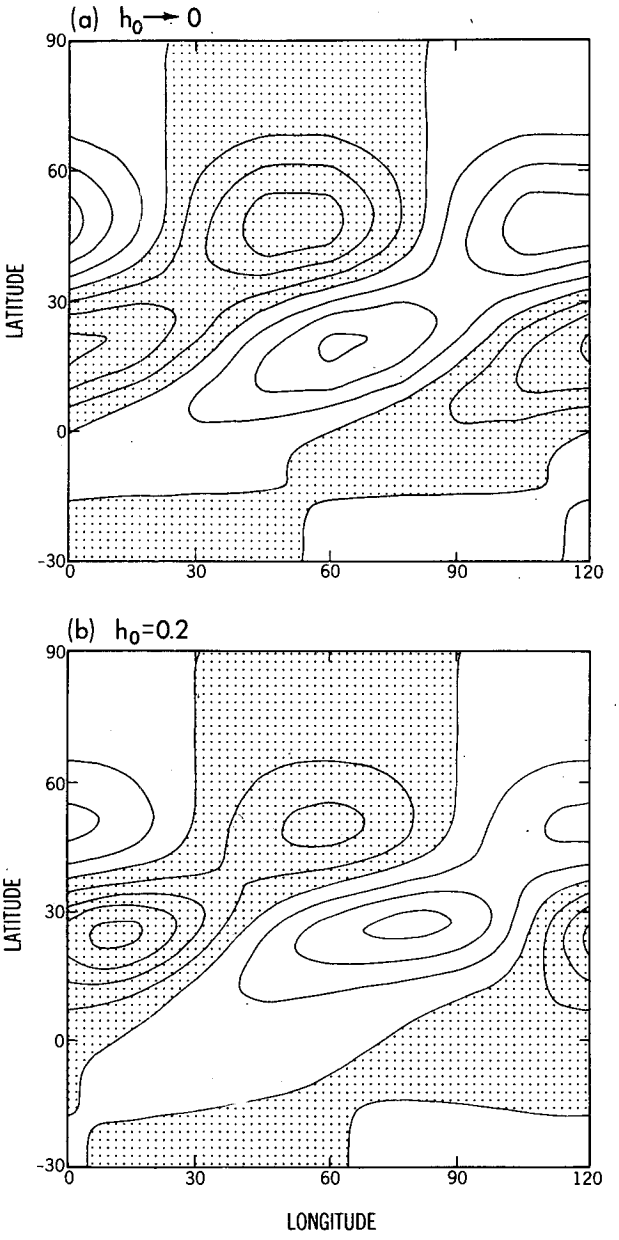

FIG. 3. The eddy streamfunction obtained from the Hadley plus the Rossby wave model (a) in the limit of infinitesimal wave forcing, and (b) for $h_0 = 0.2$. Negative values are shaded. The linear result is normalized so that the two figures would be identical if linear theory remained valid for the finite-amplitude case. The contour interval in (b) is 6×10^6 m^2 s^{-1}. The "topography" peaks at 0° and 120° longitude.

where

$$\chi(y) \equiv \int_{y_0}^{y} l(\xi)d\xi,$$

and l is the local stationary meridional wavenumber (and where both A and R are slowly varying in y), then

$$\frac{\overline{u'v'}}{(|\overline{u'^2}||\overline{v'^2}|)^{1/2}} \approx \frac{(1 - |R|^2)}{([1 + |R^2|]^2 - 4|R|^2 \cos^2(\chi_R + 2\chi))^{1/2}}, \quad (17)$$

where $R = |R| \exp(i\chi_R)$. This quantity oscillates between unity and

$$(1 - |R|^2)/(1 + |R|^2). \quad (18)$$

[See Rousteenoja (1990) for further discussion of this method of computing the reflection coefficient.] Figure 4 shows the latitudinal structure of this correlation between 10°S and 45°N for Hadley + infinitesimal wave calculations with different values of κ_M. The correlation has a structure consistent with that implied by the WKB wavefunction, so one can hope to approximate the reflection coefficient by equating the minima in this curve with (18). For $\kappa_M^{-1} = 20$ d, this estimate yields $|R| \approx 0.35$ if one uses the minimum between 15° and 30°N. The larger value further north suggests additional reflection from the region near 30°, which is plausible given the sharp structure in the vorticity gradient (Fig. 2), but cannot be trusted because of overlap with the source. The reflection coefficient increases with decreasing damping, a consequence of the changes in the zonal flow pictured in Fig. 2. As the Rayleigh damping is reduced, the absolute vorticity in the tropics approaches zero and the vorticity gradients needed for Rossby wave propagation disappear. One expects perfect reflection of an infinitesimal wave from the northern margin of the Hadley cell in the limit $\kappa_M \rightarrow 0$ (cf.

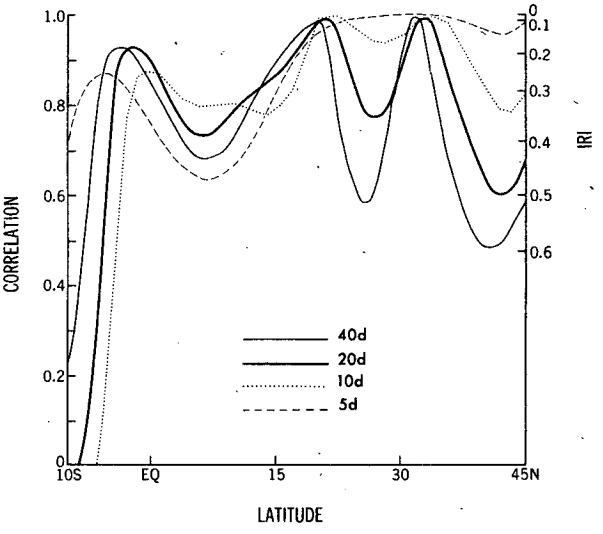

FIG. 4. The correlation coefficient between the eddy zonal and meridional velocities, for 4 values of κ_M^{-1}. From local minima in these curves one can infer the reflection coefficient shown on the right.

Platzman 1949). One expects little reflection of infinitesimal waves from the observed zonally averaged climatological profile, however, which more nearly resembles the flows with large damping in Fig. 2.

The existence of a stationary Rossby wave resonance is responsible for the presence of multiple equilibria in the model of Charney and Devore (1979), and in other similar models for stationary waves interacting with the zonal mean flow. The existence of such a resonance is, in turn, a consequence of reflection from the beta-plane channel walls. The present model can be considered a spherical version of Charney and Devore (1979) [in this sense it is similar to Legras and Ghil (1985)], but one in which the mean flow is maintained by a thermally driven Hadley cell. Therefore, it is of interest to determine if the partial reflection seen here is sufficient to produce resonant-like behavior. Figure 5 is a plot of the eddy streamfunction squared, averaged over the globe, as a function of $\Delta\Phi_e$ for κ_M^{-1} = 20 d and 10 d. As $\Delta\Phi$ is varied, U changes in strength, and one might expect to pass through a resonance in analogy with Charney and Devore. A resonance is clearly present near $\Delta\Phi_e = 1.3 \times 10^4$. Increasing κ_M damps the resonance because of the reduction in reflectivity due to the more ample vorticity gradients in low latitudes as well as the smoother vorticity gradient structure near the jet, and also because direct damping of the wave begins to play a role.

Despite this potential for resonant behavior, the present model differs fundamentally from that of Charney and Devore (1979) with regard to the distribution of the mean flow modification due to the wave.

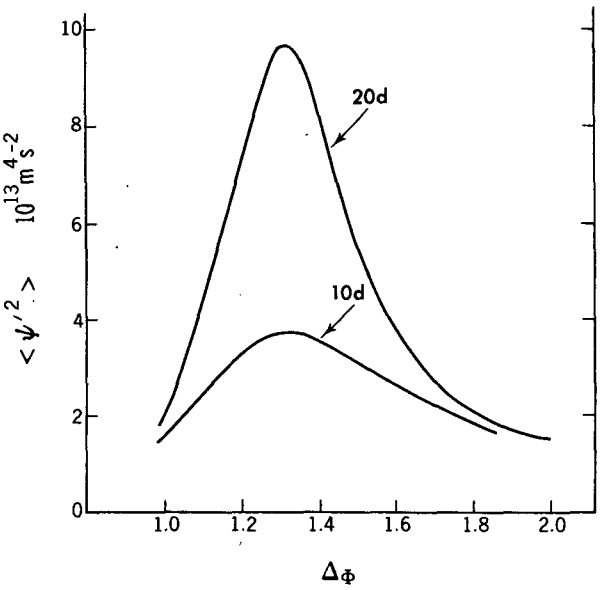

FIG. 5. Globally averaged eddy streamfunction squared, as a function of the "radiative equilibrium" height gradient, Δ_Φ, for two values of κ_M^{-1}.

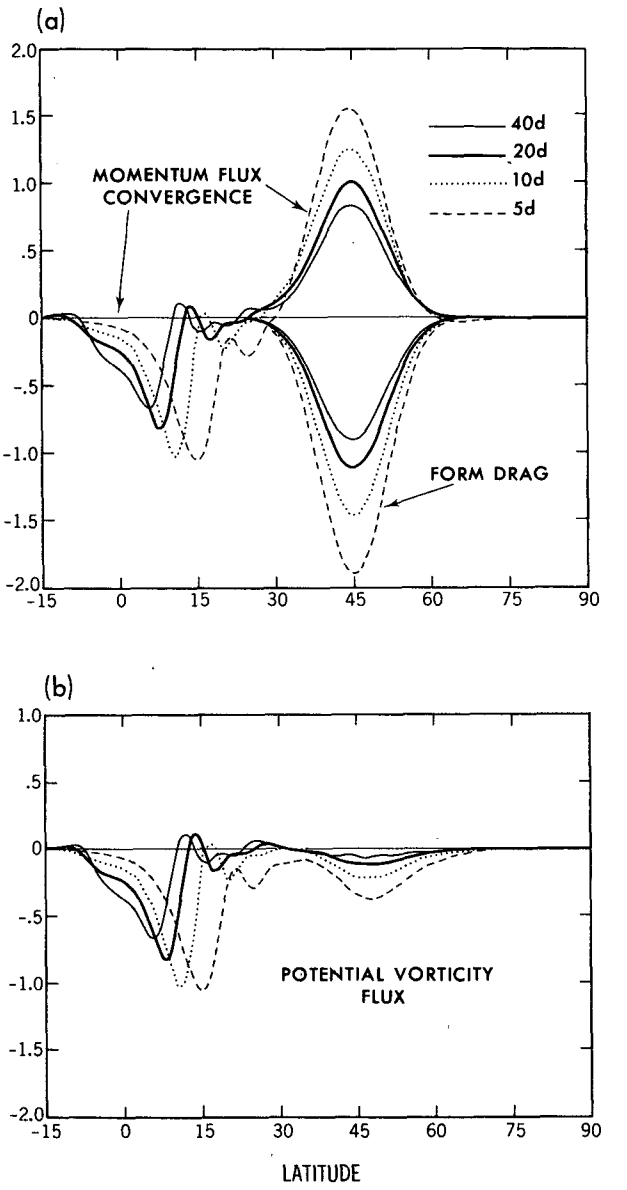

FIG. 6. (a) The stress exerted on the mean zonal flow due to the eddy momentum flux convergence and to the form drag, or mountain torque, and (b) their sum, the eddy potential vorticity flux, for infinitesimal Rossby wave forcing with the same 4 values of κ_M^{-1} as in Figs. 2 and 4. Units are $(h_0/0.1)^2$ m s^{-1} day^{-1}.

Returning to the standard parameter setting with $\Delta\Phi_e = 2 \times 10^4$, Fig. 6 shows the form drag, the eddy momentum flux convergence, and their sum, the eddy potential vorticity flux for different values of κ_M. The form drag and the momentum flux convergence nearly balance in the source region, a consequence of the nonacceleration theorem [see Eq. (20) below], so that the bulk of the potential vorticity flux occurs in low latitudes. The equatorward penetration of the momentum flux increases as the dissipation is lowered. The

form drag also has some sensitivity to the dissipation. Since the directly excited wave should have little sensitivity to damping at the smaller values of κ_M in Fig. 6, the changes in form drag likely result from changes in reflectivity and interference between the incident and reflected waves.

One can derive an expression relating $\overline{v'q'}$ to the dissipation of the wave by Rayleigh friction and diffusion and to advection of the eddy enstrophy by the mean meridional circulation. Starting with

$$\partial_t q' = -U\partial_x q' - \gamma v' - \partial_y(Vq') - \kappa_M \zeta' - \nu\nabla^4\zeta', \quad (19)$$

where $\gamma \equiv \partial_y(f + Z)$, multiplying by q' and averaging around a latitude circle, one finds for a stationary wave that

$$\gamma\overline{v'q'} = -\kappa_M\overline{q'\zeta'} - \nu\overline{q'\nabla^4\zeta'} - \overline{q'\partial_y(Vq')}. \quad (20)$$

Figure 7 shows $\overline{v'q'}$ for κ_M^{-1} = 20 d decomposed into these three contributions. The biharmonic diffusion contributes a small amount near the peak of $\overline{v'q'}$, while the contribution of Rayleigh friction is larger in low latitudes and dominant near the source. However, the less familiar term involving the meridional circulation is the largest of the three, explaining more than half of the flux where this flux is largest. A meridional flow opposed to the group velocity of a Rossby wave train, as here, retards the wave and prevents what would otherwise be deeper penetration into the tropics (see Watterson and Schneider 1987). We have confirmed that removing the effect of V on the wave results in the displacement of the peak in $\overline{v'q'}$ to the equator, the location of the critical latitude. Thus, not only is the wave influenced by the zonal flow, but also in a more subtle way, by the meridional flow as well.

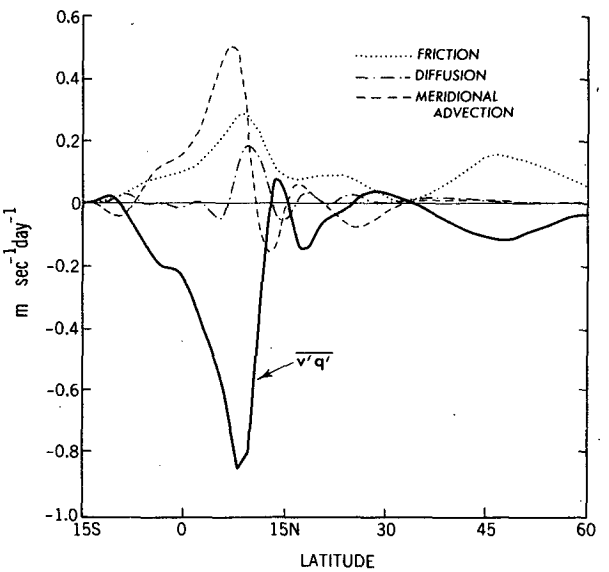

FIG. 7. Decomposition of the eddy potential vorticity flux for infinitesimal forcing and κ_M^{-1} = 20 d, into the contributions from biharmonic diffusion, Rayleigh friction, and advection by the mean meridional circulation. These terms are plotted so that their sum equals the negative of $\overline{v'q'}$. Units as in Fig. 6.

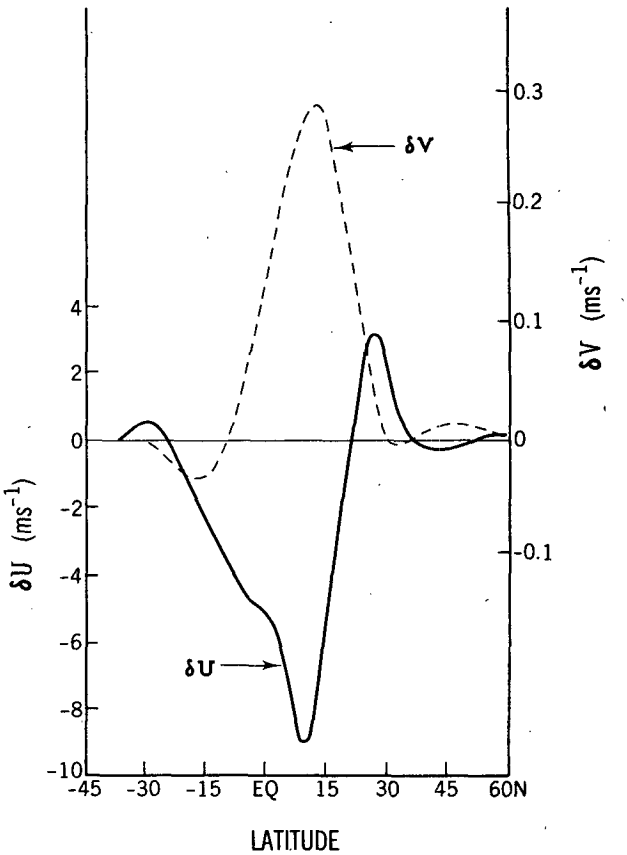

FIG. 8. The changes in the zonal mean zonal and meridional flows due to an infinitesimal Rossby wave, with κ_M^{-1} = 20 d. The changes are negligible outside of the latitude span shown. Values shown should be multiplied by $(h_0/0.1)^2$.

The Hadley ceil model's response to the eddy forcing, $\overline{v'q'}$, due to this infinitesimal wave is shown in Fig. 8. The response $(\delta U, \delta V)$, which is proportional to the square of the wave amplitude, has been normalized to correspond to $h_0 = 0.1$. While the zonal flow is decelerated in the region where $\overline{v'q'}$ is largest, there is also significant acceleration centered near 30°N. The deceleration spreads well into the Southern Hemisphere. The northern branch of the Hadley cell has been strengthened, and the zero crossing in V shifted slightly into the Southern Hemisphere.

Suppose for the moment that the steady state balance in the zonal momentum equation is simply

$$0 = fV - \kappa_M U + \overline{v'q'}. \quad (21)$$

If one also ignores the minor term quadratic in U in the V-equation, as well as the small damping term, so that

$$0 = -fU - a^{-1}\partial_\theta \Phi, \tag{22}$$

one can derive a relatively simple second-order equation for the response δV to the eddy driving:

$$f^2\delta V - \frac{\Phi_0 \kappa_M}{\kappa_T a \cos(\theta)} \frac{\partial}{\partial \theta} \frac{1}{a \cos(\theta)} \times \frac{\partial}{\partial \theta}(\cos(\theta)\delta V) = -f\overline{v'q'}. \tag{23a}$$

One can then obtain δU from

$$\kappa_M \delta U = f \delta V + \overline{v'q'} \tag{23b}$$

or

$$\delta U = \frac{\Phi_0}{f\kappa_T a \cos(\theta)} \frac{\partial}{\partial \theta} \frac{1}{a \cos(\theta)} \frac{\partial}{\partial \theta}(\cos(\theta)\delta V). \tag{23c}$$

For extratropical forcing centered at latitude θ_0 the character of the response depends on the relative magnitude of the meridional scale of the eddy forcing L_f and the scale L defined by

$$L^2 \equiv \Phi_0 \kappa_M / (f(\theta_0)^2 \kappa_T). \tag{24}$$

If $L_f \gg L$, $f\delta V \approx -\overline{v'q'}$ is the approximate solution to (23), and the eddy stress is primarily balanced by the perturbed Coriolis force. In this limit, δU is independent of κ_M and is best determined from (23c). If $L_f \ll L$, on the other hand, $\overline{v'q'}$ is primarily balanced by the Rayleigh friction. For a localized stress with scale smaller than L, the response of the meridional flow will have the scale L, resulting in acceleration of the zonal flow north and south of a localized eddy stress. In the limit of δ-function forcing, the response δU is unphysical, since it will have a δ-function singularity as well.

If we take $\theta_0 = 8°$N for our case, then $L \approx 1 \times 10^6$ m, which is comparable to the distance to the equator, so (24) must be replaced by the equatorial radius of deformation, modified once again by the ratio of mechanical to thermal damping rates:

$$L_e^4 \equiv \Phi_0 a^2 \kappa_M / (\Omega^2 \kappa_T). \tag{25}$$

For eddy stress confined within a distance L_e from the equator, as is the case in Fig. 6, the stress is primarily balanced by Rayleigh friction, while δV has the scale L_e, resulting once again in acceleration outside of the source.

Given the full zonal momentum equation (1a), the response to small eddy forcing (ignoring the very small direct effect of diffusion on the mean flow) satisfies

$$0 = (f + Z)\delta V + V\delta Z - \kappa_M \delta U + \overline{v'q'}. \tag{26}$$

If the second term in (26) is negligible, one can still derive an equation analogous to (23a), with $f^2\delta V$ replaced by $f(f + Z)\delta V$. However, if the second term plays a significant role, the order of the equation is raised and interpretation in general is less straightforward. This term becomes more important as the source becomes narrower. In the limit that $\overline{v'q'}$ approaches a δ-function, $F_0\delta(y - y_0)$, the dominant balance in the source region becomes $\delta Z\, V \approx F_0\delta(y - y_0)$, so that the zonal flow jumps by the amount $F_0/V(y_0)$ passing through y_0 in the direction of the meridional flow. Figure 9 shows the balance of terms in (26) for the present calculation. The term $\delta Z\, V$ is found to be very significant, in fact comparable to $\overline{v'q'}$ itself. The solution has something of the character of the response to a δ-function, in that $\delta Z\, V$ does balance part of the deceleration near the maximum in $\overline{v'q'}$; however, Rayleigh friction remains dominant in this region. Farther north, the primary balance is between the first two terms in (26).

In the nearly inviscid limit $\kappa_M \to 0$, an alternative explanation exists for the acceleration of the flow in the subtropics, based on the construction of Held and Hou illustrated in Fig. 10. Poleward of θ_H, $\Phi = \Phi_e$; equatorward of θ_H; Φ is in balance with the momentum conserving flow U_M (in the absence of eddy stresses) and is, therefore, determined up to an additive constant. This constant and θ_H are simultaneously determined by requiring that Φ be continuous at θ_H and that the integral of $\Phi - \Phi_e$ from the equator to θ_H vanish. If we now add a localized eddy stress, the zonal flow is reduced by an amount inversely proportional to V as it passes through this region, with the result that the geopotential gradient is weakened and θ_H is required to move poleward to satisfy the constraints (see figure). As a consequence, the zonal flow is accelerated between the unperturbed and the new Hadley cell boundaries. The intensity of the Hadley cell will

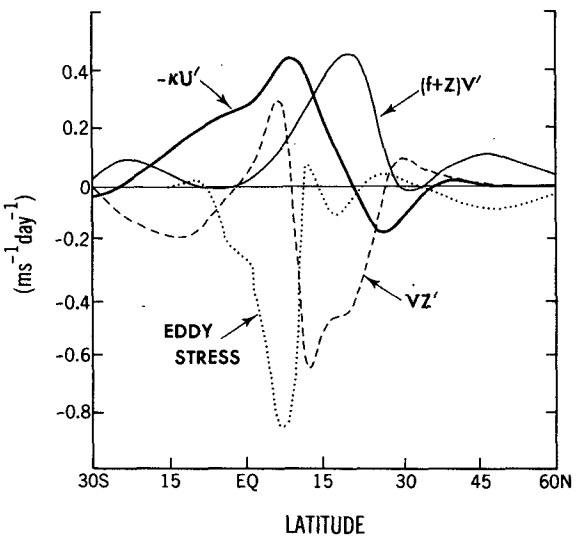

FIG. 9. The terms in the zonal momentum equation that balance the stress due to an infinitesimal Rossby wave. The prime here refers to the deviation from the state with no wave present. Units and normalization as in Fig. 6.

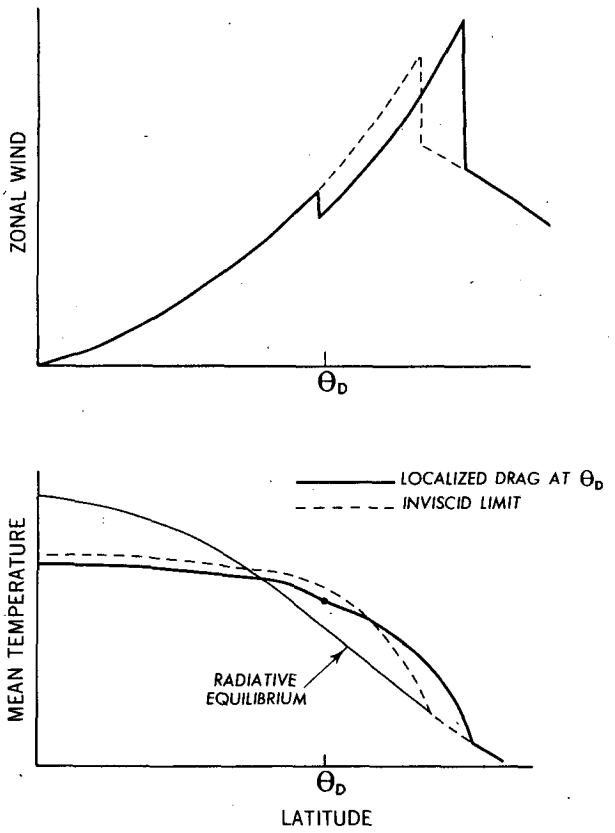

FIG. 10. A schematic of the changes in the zonal wind and mean temperature due to the addition of localized drag at the latitude θ_D to the nearly inviscid Hadley cell discussed by Held and Hou (1980).

also increase. (We are implicitly assuming that $U = 0$ at the equator; strictly speaking the addition of stress asymmetric about the equator will move the point at which $V = 0$ off the equator, creating equatorial easterlies; this will reduce the zonal winds further and add an additional slight poleward perturbation to θ_H.) Thus, in both the linear and nearly inviscid limits one expects subtropical acceleration in response to localized low latitude stress. The behavior of the present model appears to be intermediate between these nearly inviscid and dissipative limits.

At the equator, an infinitesimal eddy stress is balanced entirely by the Rayleigh friction in this model. The inclusion of vertical transport of momentum (i.e., a momentum source related to the mass source) would allow for the possibility of a balance less dependent on friction in the deep tropics.

5. Finite amplitude Rossby waves

We now examine how the eddy stress and the resulting mean flow modification change as h_0 increases. The nonlinear vorticity equation, coupled to the mean equations for V and Φ (1b, 1c), is integrated forward in time using rhomboidal 60 truncation, but retaining only those zonal wavenumbers that are a multiple of 3, the zonal wavenumber of the source. A leapfrog time step is used for all except the dissipative terms, for which a forward step is used. The integration is restarted every 30 steps to avoid time splitting. We use the parameters listed in (8), with $\kappa_M^{-1} = 20$ d once again. (With smaller damping, the approach to equilibrium slows to the point that the integrations become too time consuming. Furthermore, as the damping is reduced, the jet eventually becomes sharp enough to generate barotropic instabilities, a regime we prefer to avoid.) Steady solutions are obtained for $h_0 < 0.08$. At this point there is a bifurcation to a simple limit cycle. The solution is exactly periodic at least up to $h_0 = 0.25$. We have had difficulty obtaining stable numerical integrations for $h_0 > 0.25$, for reasons that we do not yet understand.

Figure 11 shows the evolution of the absolute vorticity through one period of the limit cycle for $h_0 = 0.2$. The system takes roughly 6 days to complete a cycle. A wave breaking event in low latitudes dominates the evolution. A tongue of low vorticity air is swept polewards, entrained into the anticyclonic flow and then dissipated, only to be regenerated 6 days later. The resulting time-mean absolute vorticity pattern is shown in the center of the figure.

The deviations from zonal symmetry of the time-mean streamfunction for this case are compared with its linear limit in Fig. 3b. The linear result has been normalized appropriately. The change in the pattern from the linear prediction is not dramatic. A shift polewards and eastwards is evident in the subtropics, with the cyclonic circulation favored slightly over the anticyclonic, and the penetration into the Southern Hemisphere is reduced. In midlatitudes, the eastward shift results in a reduction in the form drag.

Figure 12 shows the time-mean eddy potential vorticity flux for several values of h_0. The actual fluxes are plotted in (a); the fluxes have been divided by $[h_0(0.1)]^2$ in (b) for comparison with the linear prediction. The observed (stationary plus transient) eddy vorticity flux in the subtropics near the tropopause in northern winter is ≈ 2 m s^{-1} day^{-1} (Lau et al. 1981), which is obtained in this model for h_0 between 0.2 and 0.25.

The stress generated by the Rossby wave in low latitudes broadens and moves polewards as the amplitude of the wave increases. This is precisely the behavior observed by Held and Phillips (1987) in the transient decay of a disturbance excited in midlatitudes. The broadening is a natural consequence of the larger particle displacements in the breaking region that occur as the forcing amplitude increases. The poleward shift may also be related to the reduction in the mean vorticity gradient in low latitudes evident in Fig. 11 (see also Fig. 16 below), or, in the picturesque terminology

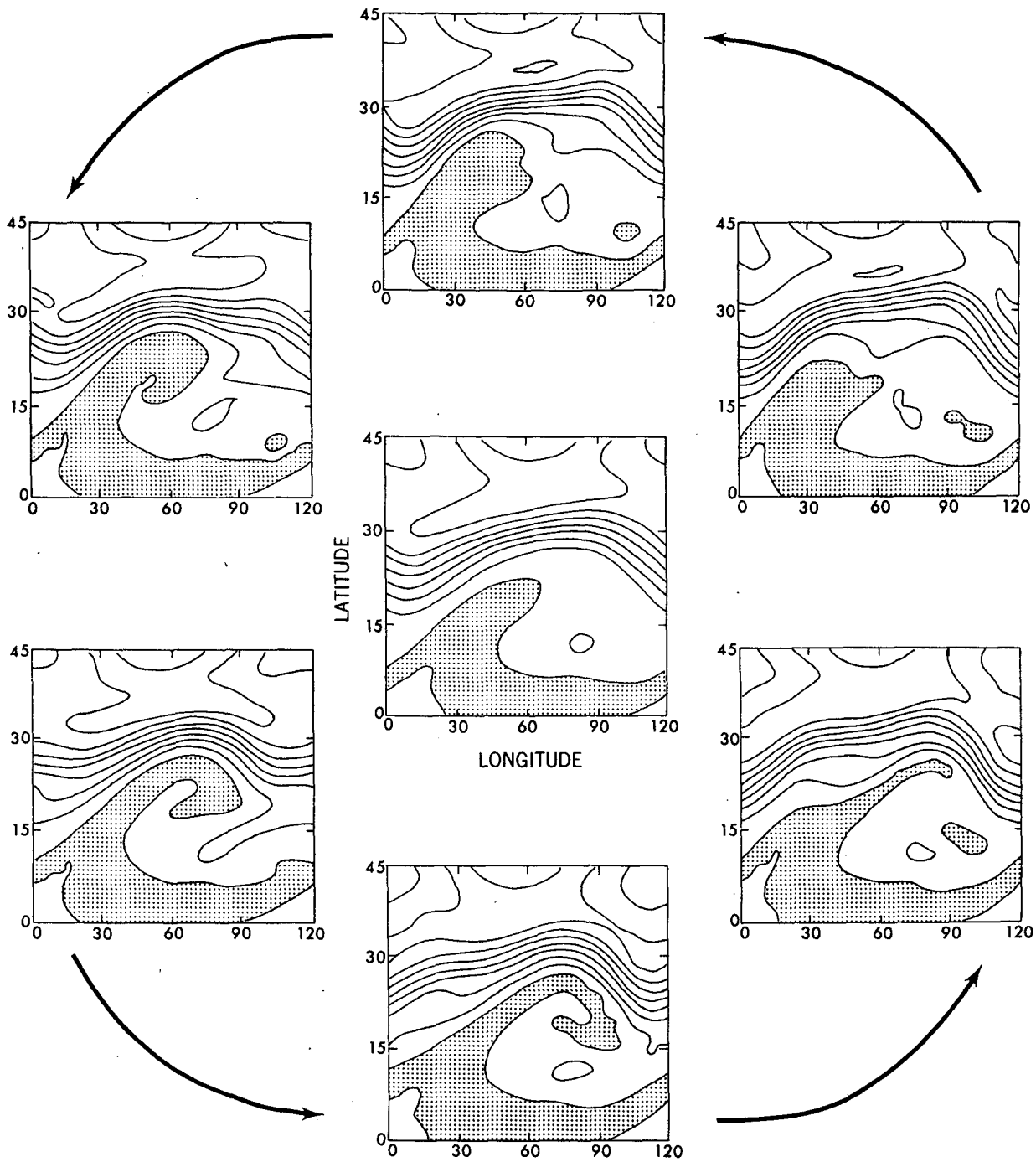

FIG. 11. The absolute vorticity field in the tropics at six equally spaced times in the periodic solution produced with $h_0 = 0.2$. The central figure is the time average. The contour interval is 1.35×10^{-5} s^{-1}. The time between snapshots is $\sim$1 day.

of McIntyre and Palmer (1984), to the generation of a "surf zone" that limits the penetration of Rossby waves.

One expects the resonant behavior seen for infinitesimal forcing to have important consequences at finite amplitude. The behavior of the model is complex. There is a transition to chaotic behavior as Δ_Φ is reduced with $h_0 = 0.2$, and the wave amplitude undergoes large fluctuations. The chaotic solutions will be described elsewhere. Behavior that is fundamentally dif-

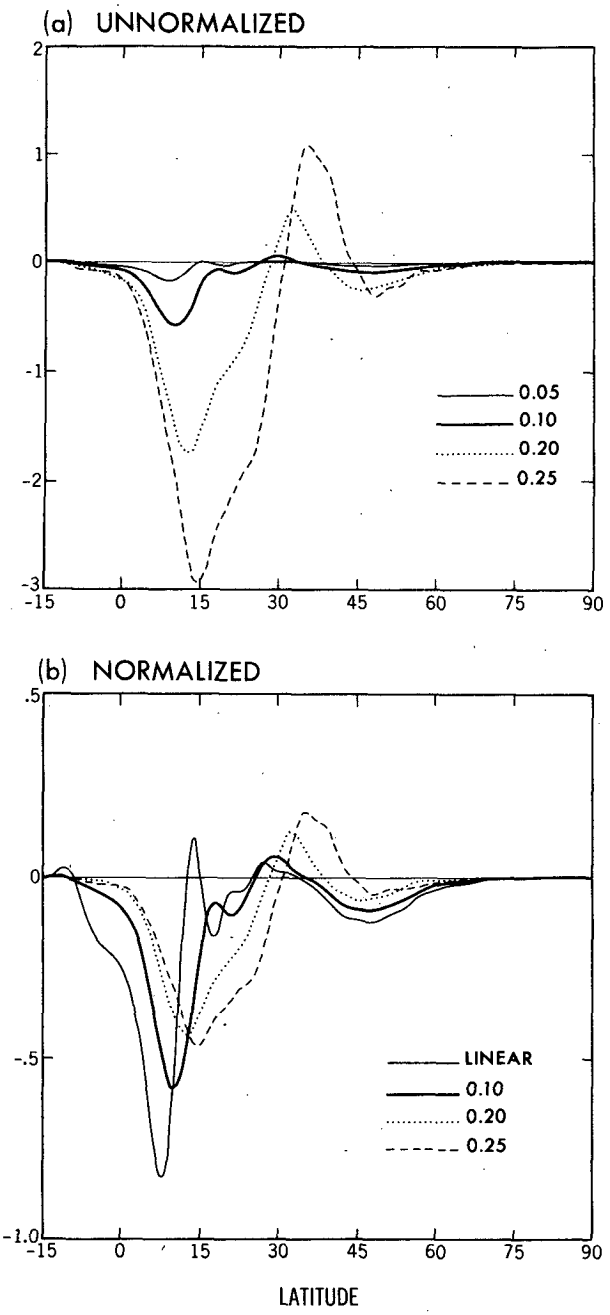

FIG. 12. (a) The time-mean eddy potential vorticity flux for four values of the forcing h_0. Units are m s^{-1} day^{-1}. In (b) the curves for the three largest amplitudes in (a) are multiplied by $(h_0/0.1)^2$ for comparison with the linear prediction.

ferent from that in Charney–Devore-like models is to be expected, since the mean-flow modification takes place primarily in low latitudes. It will be of interest to determine whether or not behavior of this model is similar to that of a spherical barotropic model with the mean flow maintained by Rayleigh friction as in Legras and Ghil (1985).

Returning to the standard parameter setting, with $\Phi_e = 2 \times 10^4$ and $\kappa_M = 20$ d, the U and V profiles obtained for $h_0 = 0.25$ are displayed in Fig. 13. The Hadley cell in the Northern Hemisphere has been strengthened by a factor of 2. Also shown is the Eulerian mean $V_e = V + \overline{v'h'}$ (see the Appendix), in which the expected development of a Farrell cell is observed. The acceleration of U in the subtropics persists as h_0 increases, and the jet shifts poleward. The maximum deceleration obtained for the largest wave forcing ($h_0 = 0.25$) is 16 m s^{-1}. If the mean flow were maintained by linear relaxation to some reference state, an e-folding relaxation time of $\approx$5 days would be needed to produce

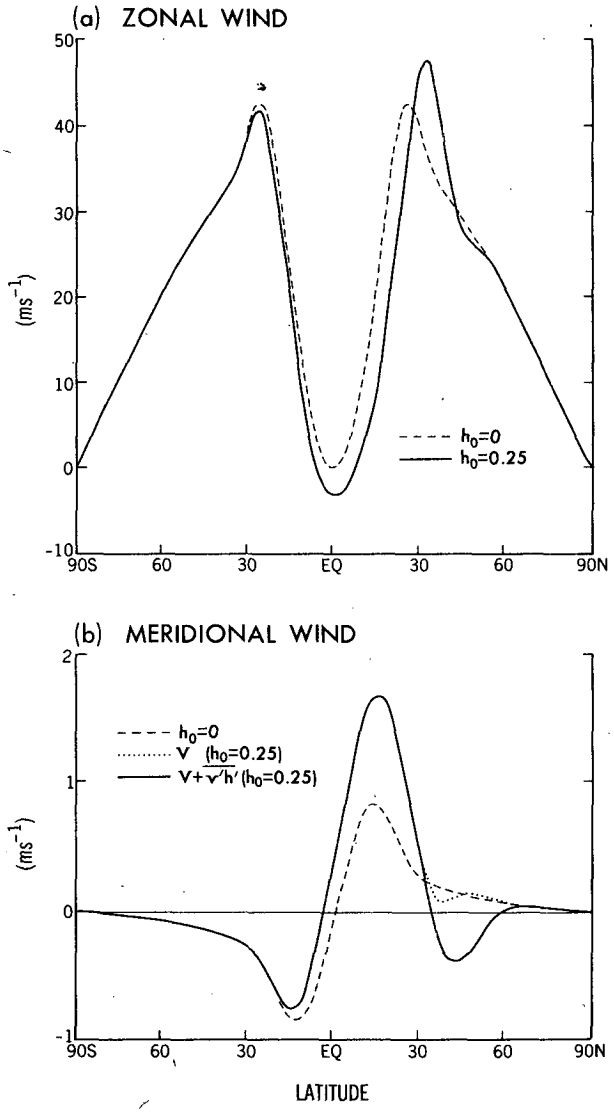

FIG. 13. The zonal mean (a) zonal and (b) meridional winds produced by the Hadley cell plus Rossby wave model with $h_0 = 0.25$, and the corresponding winds in the absence of a Rossby wave. In the region in which the forcing is nonzero in (b), the residual circulation (dotted line) and the Eulerian mean circulation (solid line) are both shown. Away from the forcing, these are identical.

a deceleration of this size, given the strength of the eddy forcing in Fig. 12. Simple linear relaxation to a prespecified flow would not produce significant subtropical acceleration, while the acceleration, in fact, is of comparable amplitude to the deceleration for large wave forcing.

In Fig. 14 the changes (δU, δV) from the flow without eddy stresses, normalized by the square of the forcing amplitude as in Fig. 12b, are presented. The low-latitude zonal-flow deceleration is seen to be reduced dramatically from the linear prediction, by a factor of 4 for $h_0 = 0.2$. The subtropical acceleration retains much of its strength, so that it becomes comparable in size to the deceleration for the larger values of h_0. The reduction in the normalized δV is less pronounced than that in δU. Further inspection of the solutions shows that the normalized form drag, and, therefore, the integrated eddy stress in low latitudes, weakens as h_0 increases, explaining a part of these reductions. The broadening of the eddy stress is also important, since this favors a mean flow response in which the Coriolis force plays a greater role, thereby reducing δU. The poleward shift of the eddy stress has the same effect since it results in a decrease in the effective deformation scale L. [We are admittedly thinking here of an equation similar to (21), which is not entirely adequate; however, we see the same qualitative behavior in calculations with larger κ_M, for which the Hadley response should more nearly correspond to that predicted by (20).]

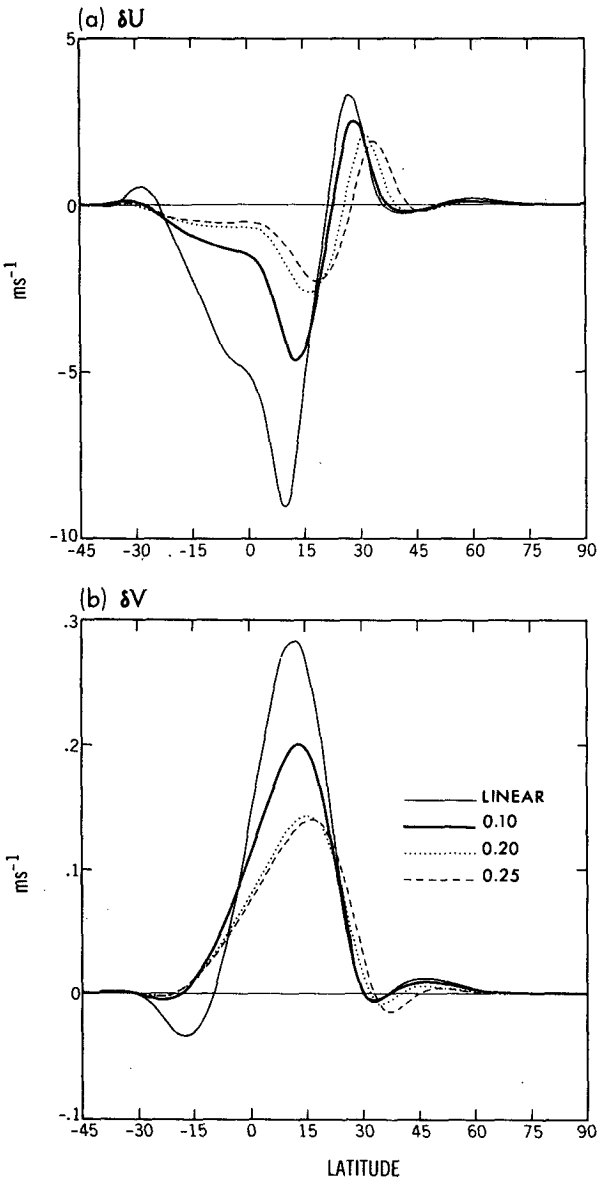

FIG. 14. The changes in zonal mean (a) zonal, and (b) meridional winds produced by Rossby waves of different amplitudes, normalized as in Fig. 12b.

The time-mean momentum budget for the case $h_0 = 0.25$ is shown in Fig. 15. This model has succeeded in producing a flow in which the eddy momentum flux divergence, rather than the arbitrarily specified Rayleigh friction, balances the Coriolis force (or $(f + Z)V$ more generally) in low latitudes. In terms of the Eulerian mean meridional flow, the model also has the approximate balance $fV_e \approx \partial_y(\overline{u'v'})$ in midlatitudes, since V is small enough that $V_e \approx \overline{v'h'}$, and since $\overline{v'h'} \approx -\overline{v'\zeta'}$. This balance, however, disguises the important fact that the eddy vorticity flux and the form drag nearly cancel, leaving the Rayleigh friction to balance the Coriolis force on the residual circulation V, just as in the unperturbed Southern Hemisphere. To remove the unrealistic dependence on the Rayleigh friction in midlatitudes, one would have to generate eddies that break at these latitudes.

6. Conclusions

A heuristic barotropic model has been constructed to describe the interactions in the upper troposphere between the Hadley cell and Rossby waves propagating into the tropics from midlatitudes. The special case is considered in which the wave forcing is stationary and has a zonal wavenumber 3 structure.

Even for infinitesimal Rossby wave forcing, the behavior of the model is more complex than one might wish:

- The distribution of the eddy stress on the mean flow is found to be strongly influenced by the mean meridional circulation.
- The response of the zonal mean flow to this infinitesimal stress includes not only the expected deceleration in low latitudes but also acceleration in the subtropics. This subtropical acceleration in response to a negative low latitude stress persists in the "nearly inviscid" Hadley cell model described by Held and Hou (1980).
- The change in the meridional advection of angular momentum $V\partial M/\partial y = -V(f + Z)$, where Z is the

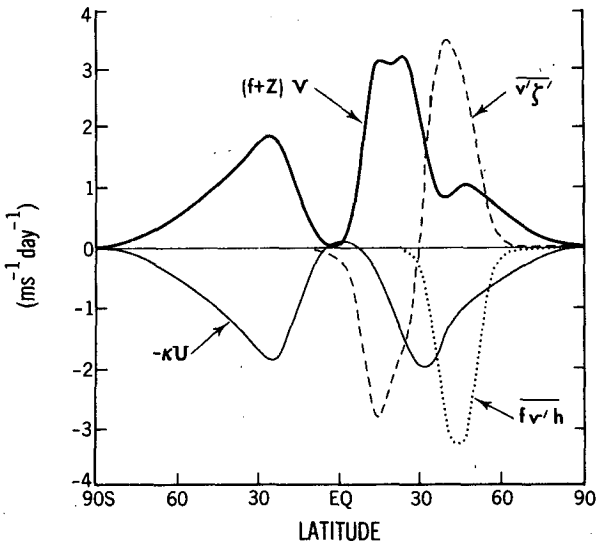

FIG. 15. The balance of terms in the zonal momentum equation, for the case $h_0 = 0.25$.

zonal mean relative vorticity, cannot simply be approximated by the change in the Coriolis force, but changes in Z are also important. As a result, the equation for the response to the infinitesimal stress is third order, rather than second order, in latitude.

- Substantial reflection of the wave propagating into low latitudes can occur, thereby providing the potential for resonant behavior. The reflection coefficient can be estimated by inspecting the latitudinal structure of the correlation between the eddy zonal and meridional velocities.

As the strength of the Rossby wave forcing is increased, the linear limit remains a useful zeroth-order guide to some of the behavior observed. Most importantly, the eddy stresses are still mainly confined to the wave absorption region in low latitudes; however, departures from the linear prediction can be striking:

- The eddy stress broadens and shifts poleward. (No quantitative method for computing the resulting distribution of the eddy stress, other than direct numerical integration, is proposed; if such a method could be found it would likely play an important role in eddy flux closure theories.)
- Due to this shift in the eddy stresses, the mean modification departs drastically from the linear prediction at wave amplitudes that yield realistic magnitudes for the low-latitude eddy-momentum flux divergence. The subtropical acceleration grows as large as the lower latitude deceleration at large wave amplitudes.
- An instability associated with wave breaking in low latitudes results in periodic flow above a critical wave forcing amplitude. (Only solutions that have the same threefold symmetry as the forcing have been examined; other instabilities could emerge when this symmetry is relaxed.) Chaotic behavior is found at parameter settings other than those emphasized in this paper, particularly near the parameter setting that produces a resonance with infinitesimal forcing.

This model can be viewed from two distinct perspectives: as a generalization of Charney–Devore type models of stationary wave–mean flow interaction, and as a model of the upper tropospheric flow in which the stationary wave is simply a surrogate for the full spectrum of Rossby waves generated in midlatitudes. From the first perspective, the distinctive feature of this model is that the bulk of the mean flow modification induced by the wave stresses occurs in low latitudes. Interesting dynamics should be associated with the resonance, but the dynamics will have a somewhat different character than that produced by models in which the mean flow is altered by the wave-induced stresses in the vicinity of the source.

One is tempted to claim, on the basis of these results, that the bulk of the mean flow modification due to the presence of a midlatitude mountain should be expected in low latitudes. In reality, mixing by baroclinic eddies is likely sufficient to create substantial mean flow modification at the latitude of the source as well.

From the second perspective, the model has interesting deficiencies. The nearly inviscid Hadley flow has no vorticity gradient in low latitudes. Observations show substantial gradients, consistent with a zonal flow that is far weaker than the momentum conserving limit in the subtropics. It is natural to assume that it is the mixing by large-scale eddies that generates these gra-

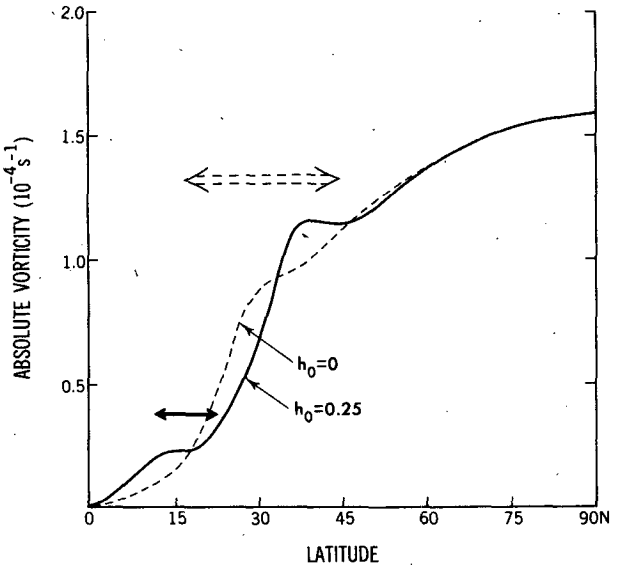

FIG. 16. The zonal mean absolute vorticity produced with $h_0 = 0.25$ compared with that produced when there is no Rossby wave. The solid arrow illustrates the mixing that produces this modification. The dotted arrow illustrates the mixing that would be needed to increase gradients in low latitudes.

dients; however, no significant creation of low latitude vorticity gradients occurs in the present calculation. Figure 16 compares the time and zonal mean absolute vorticity distribution produced with large Rossby wave forcing ($h_0 = 0.25$) with that produced by the purely zonally symmetric model. The initial vorticity gradients have simply been reduced further in the region, marked by the solid arrow, in which substantial mixing has occurred. In order to increase the low latitude gradients, it is clear that the eddies have to take some of the high vorticity air that initially resides poleward of the jet and transfer it into low latitudes, as indicated by the dotted arrow in the figure. Such behavior cannot realistically be expected from a single steady wave in the troposphere; more plausibly, this mixing would have a diffusive character, in which a spectrum of eddies produce partially overlapping mixing events. It would be of interest to try to generate mixing of this character in the present barotropic model, using parameters for which low latitude vorticity gradients in the axisymmetric flow are very small. In such a model, the eddies propagating across the subtropics would be themselves creating the vorticity gradients that allow for the possibility of propagation.

APPENDIX

Zonal-Mean Shallow Water Equations

For the full shallow water equations, the evolution equations for a zonal mean flow driven by eddy fluxes are

$$\partial_t U = (f + Z)V + \overline{v'\zeta'}, \tag{A1a}$$

$$\partial_t V = -fU - \partial_y \Phi - \partial_y(\overline{v'^2})/2 \tag{A1b}$$

$$\partial_t \Phi = -\partial_y(V\Phi + \overline{v'\phi'}), \tag{A1c}$$

where ϕ' is the eddy geopotential. To convert to the notation of the text, set $\phi' = -\Phi_0 h'$. (We ignore the spherical geometry to simplify the discussion.) Defining the residual circulation

$$V^* \equiv V + \overline{v'\phi'}/\Phi \tag{A2}$$

and taking Φ to be a constant (Φ_0), we have

$$\partial_t U = (f + Z)V^* + \overline{v'q'}, \tag{A3a}$$

$$\partial_t V^* = -fU - \partial_y \Phi - \partial_y(\overline{v'^2})/2 - \partial_t(\overline{v'\phi'})/\Phi_0 \tag{A3b}$$

$$\partial_t \Phi = -\partial_y(\Phi_0 V^*), \tag{A3c}$$

where

$$\overline{v'q'} = \overline{v'\zeta'} - (f + Z)\overline{v'\phi'}/\Phi_0. \tag{A4}$$

If one ignores the two last terms on the right-hand side of (A3b) and the contribution of Z as compared with f in (A4), these equations are identical to those used in the text (after reintroducing spherical geometry and Rayleigh friction). Therefore, V in (1) should be interpreted as the residual circulation V^*. The neglect of the final two terms in (A3b) is justified as long as geostrophic balance is a good approximation for the zonal flow, as it is in all the calculations described in the text.

REFERENCES

Andrews, D. G., 1983: A finite-amplitude Eliassen–Palm theorem in isentropic coordinates. *J. Atmos. Sci.*, **40**, 1877–1883.

——, and M. E. McIntyre, 1976: Planetary waves in horizontal and vertical shear: the generalized Eliassen–Palm relation and mean flow acceleration. *J. Atmos. Sci.*, **33**, 2031–2048.

Charney, J. G., and J. G. DeVore, 1979: Multiple flow equilibria in the atmosphere and blocking. *J. Atmos. Sci.*, **36**, 1205–1216.

Edmon, H. J., Jr., B. J. Hoskins and M. E. McIntyre, 1980: Eliassen–Palm cross-sections for the troposphere. *J. Atmos. Sci.*, **37**, 2600–2616; see also Corrigendum, 1981, *J. Atmos. Sci.*, **38**, 115.

Held, I. M., and B. J. Hoskins, 1985: Large-scale eddies and the general circulation of the troposphere. *Advances in Geophysics*, Academic Press, 3–31.

——, and A. Y. Hou, 1980: Nonlinear axially symmetric circulations in a nearly inviscid atmosphere. *J. Atmos. Sci.*, **37**, 515–533.

——, and P. J. Phillipps, 1987: Linear and nonlinear barotropic decay on the sphere. *J. Atmos. Sci.*, **44**, 200–207.

——, and M. J. Suarez, 1978: A two-level primitive equation atmospheric model designed for climatic sensitivity experiments. *J. Atmos. Sci.*, **35**, 206–229.

Hou, A. Y., 1984: Axisymmetric circulations forced by heat and momentum sources: a simple model applicable to the Venus atmosphere. *J. Atmos. Sci.*, **41**, 3437–3455.

Juckes, M., 1989: A shallow water model of the winter stratosphere. *J. Atmos. Sci.*, **46**, 2934–2955.

Lau, N. C., G. H. White and R. L. Jenne, 1981: Circulation statistics for the extratropical Northern Hemisphere based on NMC analyses. NCAR Tech. Note NCAR/TN-1171+STR, 138 pp.

Legras, B., and M. Ghil, 1985: Persistent anomalies, blocking, and variations in atmospheric predictability. *J. Atmos. Sci.*, **42**, 433–471.

Lindzen, R. S., and A. Y. Hou, 1988: Hadley circulation for zonally averaged heating centered off the equator. *J. Atmos. Sci.*, **45**, 2416–2427.

McIntyre, M. E., and T. N. Palmer, 1984: The "surf zone" in the stratosphere. *J. Atmos. Terr. Phys.*, **46**, 825–850.

Neelin, J. D., and I. M. Held, 1987: Modeling tropical convergence based on the moist static energy budget. *Mon. Wea. Rev.*, **115**, 3–12.

Palmen, E., and C. W. Newton, 1969: *Atmospheric Circulation Systems*. Academic Press, 603 pp.

Platzman, G., 1949: The motion of barotropic disturbances in the upper troposphere. *Tellus*, **1**, 53–64.

Rousteenoja, K., 1989: Simulation of the partial reflection by the critical latitude with a linear model. Part I: Methods of regulating the reflectivity. *J. Atmos. Sci.*, **46**, 3487–3504.

Salby, M. L., R. R. Garcia, D. O'Sullivan, and J. Tribbia, 1990: Global transport calculations with an equivalent barotropic model. *J. Atmos. Sci.*, **47**, 188–214.

Schneider, E. K., 1977: Axially symmetric steady state models of the basic state for instability and climate studies. Part II: Nonlinear calculations. *J. Atmos. Sci.*, **34**, 280–296.

——, 1983: Martian great dust storms: Interpretive axially symmetric models. *Icarus*, **55**, 302–331.

Watterson, I. G., and E. K. Schneider, 1987: The effect of the Hadley circulation on the meridional propagation of stationary waves. *Quart. J. Roy. Meteor. Soc.*, **113**, 779–813.